

Kinetic study and thermodynamic equilibrium modeling of the Co(II) and Mn(II) bioadsorption using the *Rhodococcus opacus* strain

<http://dx.doi.org/10.1590/0370-44672020750119>

Amanda M. Rodrigues Pimentel^{1,4}

<https://orcid.org/0000-0002-1260-5299>

Patricia Reynoso Quispe^{2,5}

<https://orcid.org/0000-0002-9202-475X>

Rita J. Cabello Torres^{3,6}

<https://orcid.org/0000-0002-9965-9678>

Lorgio G. Valdiviezo Gonzales^{4,7}

<https://orcid.org/0000-0002-8200-4640>

Carlos A. Castañeda Olivera^{3,8}

<https://orcid.org/0000-0002-8683-5054>

Antonio Gutiérrez Merma^{1,9}

<https://orcid.org/0000-0001-9218-2566>

Iranildes Daniel dos Santos^{1,10}

<https://orcid.org/0000-0001-5493-1079>

Maurício Leonardo Torem^{1,11}

<https://orcid.org/0000-0002-2674-9349>

¹Pontifícia Universidade Católica do Rio de Janeiro – PUC-Rio, Departamento de Engenharia Química e de Materiais, Rio de Janeiro, Rio de Janeiro - Brasil.

²Universidad de Ingeniería y Tecnología - UTEC, Lima - Perú.

³Universidad César Vallejo - UCV, Escuela Profesional de Ingeniería Ambiental, Lima - Perú.

⁴Universidad Tecnológica del Perú - UTP, Lima - Perú.

E-mails: ⁴manda_pimentel@hotmail.com,

⁵preynoso14@gmail.com, ⁶rcabellot@hotmail.com,

⁷lorgiovaldiviezo@gmail.com, ⁸caralcaseo@gmail.com,

⁹anguz21@hotmail.com, ¹⁰iranildes.santos@itv.org,

¹¹torem@puc-rio.br

Abstract

Microbial biomass is considered a renewable and environmentally friendly resource. Thus, the research conducted a kinetic study and thermodynamic equilibrium modeling of the cobalt (Co) and manganese (Mn) bioadsorption process using the *Rhodococcus opacus* (RO) strain as a biosorbent. The inactive biomass subjected to 0.1 M NaOH pretreatment was brought into contact with synthetic solutions of Co and Mn. The experimental data for the Co(II) and Mn(II) bioadsorption process were fit to the Langmuir model with k_{ads} of 0.65 and 0.11 L.mg⁻¹, respectively. A better statistical fit was also obtained for the pseudo-second order kinetic model ($R^2_{Co(II)} = 0.994$ and $R^2_{Mn(II)} = 0.995$), with 72.3% Co(II) and 80% Mn(II) removals during the first 10 min. In addition, a higher affinity of RO for the Co(II) ion was observed, with maximum uptake values of 13.42 mg.g⁻¹; however, a higher adsorption rate was observed for Mn(II) ion ($k = 0.21$ g.mg⁻¹.min⁻¹ at 318 K). The bioadsorption process was spontaneous and dependent on temperature, being endothermic and irreversible for the Co(II) ion ($\Delta H = 2951.91$ J.mol⁻¹) and exothermic and reversible for the Mn(II) ion ($\Delta H = -2974.8$ J.mol⁻¹). The kinetic and thermodynamic equilibrium modeling allowed to identify the main mechanisms involved in the biosorption process of both metals.

keywords: biosorption, kinetic, thermodynamic, cobalt, manganese.

1. Introduction

Some metals such as cobalt (Co) and manganese (Mn), belonging to the group of so-called microelements are considered essential because they are related to biochemical and physiological functions in humans, animals and plants; however, their requirement is in low concentrations (Hejna *et al.*, 2018). Excessive exposure of these microelements in high concentrations has been linked to cellular and systemic disorders, representing a considerable source of contamination (Rossi *et al.*, 2014). Symptoms related to Co contamination are hair loss, vomiting, bleeding, diarrhea, vasodilation, cardiomyopathy, coma and even sterility and death (Ozdemir *et al.*, 2020; Thirulogachandar *et al.*, 2014). Meanwhile, Mn contamination causes drowsiness, weakness, emotional disturbances, recurrent leg cramps and paralysis (Thirulogachandar *et al.*, 2014).

Co is present in wastewater from nuclear and mining-metallurgical plants, electroplating processes, paints, pigments and the electronics industry (Al-Shahrani, 2014). While Mn comes from the ferrous metallurgical, chemical, food electrochemical and pharmaceutical industries (Patil *et al.*, 2016). Both pollutants are present in wastewater from lithium batteries (Qiao *et al.*, 2020) and purified terephthalic acid (PTA) production, and in the petrochemical industry (Lin *et al.*, 2020).

Technologies related to the removal of heavy metals from contaminated ef-

fluents include chemical precipitation, ultrafiltration, ion exchange, reverse osmosis, electrowinning and phytoremediation. All of the above techniques have several disadvantages associated with them, such as low removal efficiency, sludge generation, energy requirements and very high reagent costs, among others (Beni and Esmaeili, 2020; Kanamarlapudi *et al.*, 2018). However, the use of low-cost bioadsorbent may be an alternative (Li *et al.*, 2019).

The use of different bacterial species has shown potential for industrial applications (Aryal, 2021). (Matsushita *et al.*, 2018) exploited the formation of biogenic manganese oxide (BioMnOx) by bacterial action to remove the metal. Likewise, (Cheng *et al.*, 2017) developed a pilot-scale biofilter using *Crenothrix* species to remove Mn(II) present in groundwater. On the other hand, (Khraisheh, Al-Ghouti e AlMomani, 2020) treated Co(II)-contaminated industrial wastewater by bioadsorption with *P. putida*. Similarly, (Dobrowolski *et al.*, 2019) and (Abu Hasan *et al.*, 2016) employed *Rhodococcus opacus* and *B. cereus* species to remove Pb(II) ($q_{\max} = 86.96 \text{ mg.g}^{-1}$) and Mn(II) ($q_{\max} = 34.76 \text{ mg.g}^{-1}$), respectively.

Bioadsorption is defined as a passive and metabolically simple physicochemical process involving the use of previously inactive adsorbents of biological origin that have demonstrated high metal removal efficiency and do not generate solid residues or toxic substances during operation.

Furthermore, this process is simple to operate, low-cost, highly efficient, does not increase chemical oxygen demand (COD), is environmentally friendly and allows regeneration of the biosorbent. (Chojnacka, 2010; Costa and Tavares, 2016).

It is common to compare the adsorption capacity between different types of biosorbents, as well as the affinity of different substances for biosorbents by means of adsorption isotherms. (Fomina e Gadd, 2014). Some isotherm models even describe the mechanism of the bioadsorption process and the distribution at equilibrium. Among the most commonly used isotherms are Langmuir, Freundlich and Temkin. (Beni and Esmaeili, 2020; Kanamarlapudi *et al.*, 2018).

The kinetic study of the bioadsorption process indicates the speed with which the pollutants are removed from the aqueous medium, and among the variety of models, the most commonly used are the pseudo-first order and pseudo-second order (Beni and Esmaeili, 2020; Calero *et al.*, 2009). Therefore, the research carried out a kinetic study and thermodynamic equilibrium modeling of the Co(II) and Mn(II) bioadsorption using the *Rhodococcus opacus* (RO) strain. For this purpose, the influence of time and temperature on the bioadsorption process was studied, and the experimental data were evaluated using the pseudo-first order and pseudo-second order kinetic models, as well as the Langmuir and Freundlich isotherms.

2. Materials and methods

2.1 Bacteria and obtaining the bioadsorbent

The RO bacteria was acquired from the André Tóselo Foundation, Sao Paulo, Brazil. It was cultivated in a liquid medium composed of 10 g.L^{-1} of glucose, 5 g.L^{-1} of peptone, 3 g.L^{-1} of malt extract and 3 g.L^{-1} of yeast extract, at pH 7.2. The incubation was carried

out at 28°C and 125 rpm for 72 h in a Cientec incubator (CT-712, Brazil). Subsequently, the cellular biomass was concentrated, quantified and stored according to the methodology described by Pimentel (2011).

To obtain the bioadsorbent, the

biomass was treated with a 0.1M NaOH solution, considering a ratio of 30 ml of NaOH solution per 100 ml of biomass. After stirring, the biomass was washed with deionized water and the pH was adjusted with 0.1M HCl solutions.

2.2 Preparation of Co(II) and Mn(II) solutions

A solution of 500 ml was prepared for each metal studied. For this purpose, the reagents cobalt(II) chloride hexahydrate ($\text{CoCl}_2 \cdot 6\text{H}_2\text{O}$; purity, 98%) and manganese sulfate monohydrate ($\text{MnSO}_4 \cdot \text{H}_2\text{O}$; purity, 98.01%) from Merck, Germany, were used. Subsequently, the standard solution was diluted to obtain the desired concentrations. For the ther-

modynamic and kinetic study of Co(II) bioadsorption, Co(II) (42 mg.L^{-1}) and biomass (4 mg.L^{-1}) solutions were used at pH 7. Meanwhile, for Mn(II) bioadsorption, Mn(II) (5 mg.L^{-1}) and biomass (3 mg.L^{-1}) solutions were used at pH 5. The contact time varied from 10 to 180 minutes, evaluated at 298 K (25°C), 308 K (35°C) and 318 K (45°C). The initial

metal concentration, biomass concentration and pH values correspond to the optimum values obtained in a previous study (Pimentel, 2011).

The concentrations of both metals were determined with an atomic absorption spectrophotometer (Perkin-Elmer; model 1100B, USA), considering a margin of error of 5% in the results obtained.

2.3 Kinetic study

The pseudo-first and pseudo-second order models are the most common and are used to explain the adsorption of met-

als using biological material.

The linear form of the pseudo-first order (Kowanga *et al.*, 2016) and pseudo-

second order (Ho and McKay, 1999) model are presented in Equation 1 and Equation 2, respectively.

$$\log(q_e - q_t) = \log(q_e) - \left(\frac{k_1}{2.303}\right)t \quad (1)$$

$$\frac{t}{q_t} = \frac{1}{K_2 q_e^2} + \frac{t}{q_e} \quad (2)$$

Where: K_1 (min^{-1}) and K_2 ($\text{g.mg}^{-1}.\text{min}^{-1}$), are adsorption rate constants; q_e (mg.g^{-1}), is the

amount of metal adsorbed per amount of biomass in equilibrium, q_t (mg.g^{-1}) is the amount

of metal adsorbed per amount of biomass at time t and t , is the adsorption time.

2.4 Thermodynamic equilibrium modeling

The thermodynamic equilibrium modeling was carried out using the Langmuir and Freundlich isotherms.

Langmuir isotherm assume adsorption in monolayers on the biosorbent surface and can be expressed by the

$$\frac{C}{q_e} = \frac{1}{q_{\max} K_{\text{ads}}} + \frac{C}{q_{\max}} \quad (3)$$

Where: q_e (mg.g^{-1}), is the amount of metal retained in the adsorbent at equilibrium; q_{\max} (mg.g^{-1}), is the Langmuir parameter related to the adsorption capacity;

K_{ads} (L.mg^{-1}), is the Langmuir constant and C (mg.L^{-1}), is the concentration of the ion in the solution at equilibrium.

Likewise, the dimensionless constant

following linearized equation (Crittenden *et al.*, 2012):

R_L is obtained by Equation 4 and is known as the separation factor or equilibrium parameter, and indicates the form and nature of the process (Weber and Chakravorti, 1974).

$$R_L = \frac{1}{1 + K_{\text{ads}} C_i} \quad (4)$$

The Freundlich isotherm explains a physical adsorption and is expressed by Equation 5 (Edzwald, 2011):

$$\log q = \log k_f + \frac{1}{N} \log C \quad (5)$$

Where: K_f and N , are the empirical constants that represent the adsorption capacity and affinity or adsorption intensity to metals.

3. Results and discussion

3.1 Influence of the time and the temperature

Figure 1-a and Figure 1-b show a rapid adsorption of metal ions in the first 10 minutes for a temperature of 298 K, reaching removal values greater than 50%. In the case of Co(II) ion, the uptake increases as the temperature increases, and remains almost constant after 10 minutes because equilibrium is reached. On the contrary, it is perceived with the Mn(II) ion, where the highest

uptake and removal are obtained at 298 K, with values of 1.07 mg.g^{-1} and 79.9%, respectively.

Bioadsorption can involve two phases, the initial phase where rapid adsorption occurs through mechanisms of physical adsorption or ion exchange, and the other phase refers to a slow adsorption that could involve complex formation, micro precipitation or satu-

ration of active sites (Esmaeili and Beni, 2015). On the other hand, temperature can have a positive or negative effect on the bioadsorption process, increasing or decreasing the adsorption capacity (Kanamarlapudi *et al.*, 2018). Additionally, increases in temperature can improve removal but can also cause structural damage to the bioadsorbent (Park *et al.*, 2010).

3.2 Langmuir and Freundlich isotherms

The experimental data of Co(II) and Mn(II) bioadsorption fitted well to both models evaluated (Langmuir, Fig. 1-c and Freundlich, Fig. 1-d). However, the best correlations were obtained with the Langmuir

model, with correlation coefficients (R^2) of 0.987 and 0.995 for Co(II) and Mn(II), respectively. This indicates that metal adsorption occurs in monolayers and at specific and uniform sites in the biomass,

considering that metals can chelate with chelating effect groups on the biomass surface (Altıntig *et al.*, 2017). The Langmuir (q_{\max} and K_{ads}), Freundlich (K_f and n_f) and R_L separation parameters are shown in Table 1.

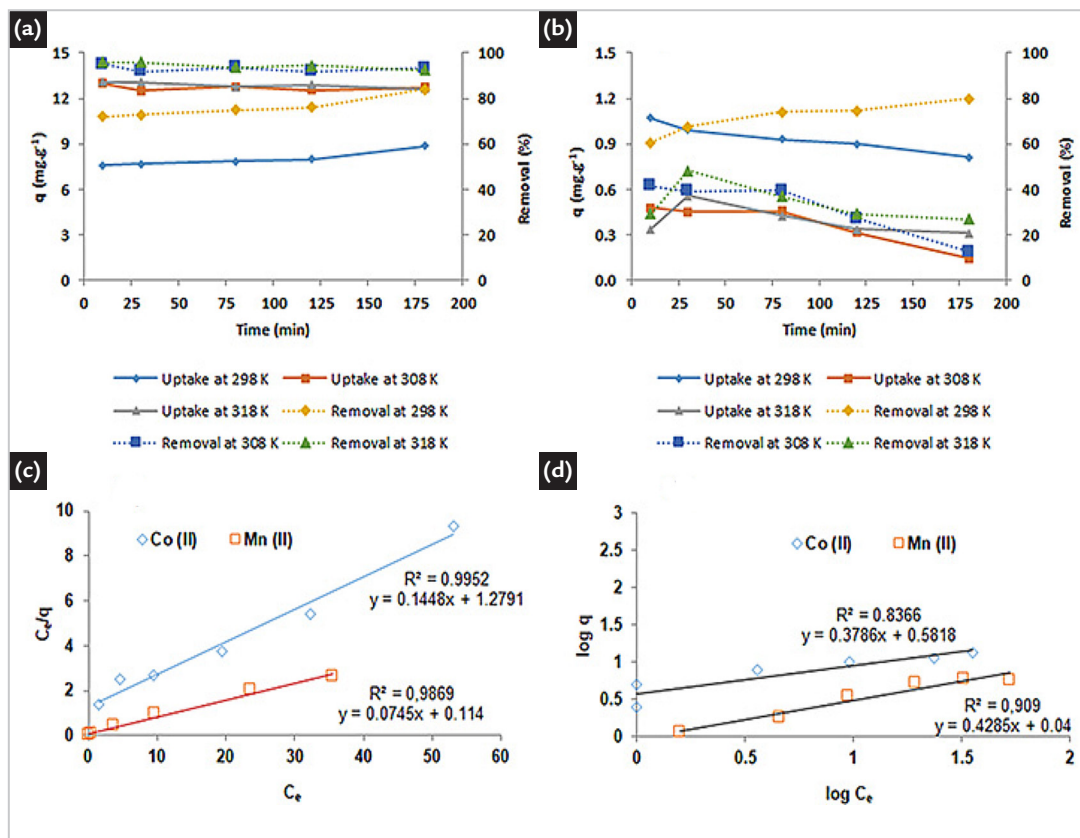


Figure 1 - a) Influence of time and temperature on uptake and removal of Co(II), b) Influence of time and temperature on uptake and removal of Mn(II), c) Langmuir isotherm for Co(II) and Mn(II) bioadsorption and d) Freundlich isotherm for Co(II) and Mn(II) bioadsorption.

Table 1 - a) Langmuir and Freundlich isotherm constants for Co(II) and Mn(II) bioadsorption and b) R_L parameters for Co(II) and Mn(II) bioadsorption.

a)	Metal	Langmuir			Freundlich		
		q_{max} (mg.g ⁻¹)	K_{ads} (L.mg ⁻¹)	R^2	K_F (L.mg ⁻¹)	n_F	R^2
	Co(II)	13.42	0.65	0.987	0.24	2.64	0.84
	Mn(II)	6.91	0.11	0.995	1.4	2.33	0.91

b)	Metal	Initial concentration (mg.L ⁻¹)							
		5	10	20	35	50	70	90	120
	Co(II)	0.234	0.133	0.071	0.042	0.03	0.021	0.017	0.013
	Mn(II)	0.639	0.469	0.306	0.202	0.15	0.112	0.089	0.069

From the data presented in Table 1-a, a greater affinity of the RO biomass for the Co(II) ion than the Mn(II) ion is observed with bioadsorption capacity values of 13.42 and 6.91 mg.g⁻¹, respectively. It was also observed that the K_{ads} and K_F constants of the Langmuir and Freundlich models are higher for Co(II) bioadsorption due to the higher uptake of this metal. (Fathollahi *et al.*, 2021) reported that 30.3% of Mn(II) bioadsorption investigations using *Bacillus sp.* achieved adsorption capacities higher than 98.12 mg.g⁻¹. Meanwhile, *B. cereus* species achieved a

maximum Mn(II) adsorption capacity of 19.27 mg.g⁻¹, following the Langmuire model ($R^2 = 0.927$) (Abu Hasan *et al.*, 2016). Similarly, *Rhodococcus opacus* applied to remove other metals such as Pb(II) and Cd(II) followed the Langmuir model ($R^2 = 0.99$), achieving adsorption capacities of 86.96 and 46.73 mg.g⁻¹, respectively (Dobrowolski *et al.*, 2019).

On the other hand, the Langmuir isotherm can be expressed through the constant R_L , called the separation factor or equilibrium parameter. If $R_L > 1$, the bioadsorption process is unfavorable;

$0 < R_L < 1$, the process is favorable; $R_L = 0$, the process is classified as irreversible and $R_L = 1$, represents linearity (Vilvanathan e Shanthakumar, 2015). Therefore, according to the results presented in Table 1-b, the R_L values obtained varied between 0 and 1, indicating that the bioadsorption process is favorable for the removal of both metal ions.

Similar results were obtained in the investigations carried out by Din *et al.* (2013) and Vilvanathan and Shanthakumar (2015) for the adsorption of Co(II), using *Saccharum bengalense*

and *Chrysanthemum indicum*, respectively. Likewise, Zhang *et al.* (2014) and

Huang *et al.* (2018) obtained favorable results in the adsorption of Mn(II) using

biomass of rice husk and *Ralstonia pickettii*, respectively.

3.3 Kinetic study

Figure 2-a shows the Co(II) and Mn(II) concentrations as a function of time, distinguishing two stages of bioadsorption. The first one occurs in the first 10 min of the process and corresponds to a fast adsorption with a rising behavior for both metal ions, and the second stage occurs after 10 min with a slow adsorption and a different behavior for each metal ion. According to Hamidpour *et al.* (2018), fast bioadsorption with high metal removal involves physical and chemical adsorption and ion exchange, and slower adsorption involves other adsorption mechanisms, such as microprecipitation and complex formation.

In the bioadsorption of Co(II), a removal of 72.3% is reached in the first 10 minutes of the process, and subsequently, the adsorption is slow and removal values of 84.2% are obtained in 180 minutes. Meanwhile, in the bioadsorption of

Mn(II), a high removal (80%) is observed in the first 10 minutes, subsequently the adsorption decreases which increases the concentration of metal ions in the solution. This behavior can be explained by the high solubility of Mn(II) in aqueous media (Bhattacharya and Elzinga, 2018).

The results of the pseudo first and second order kinetic analysis are presented in Figure 2-b and Figure 2-c, respectively. Both models were fit to the experimental data of Co(II) and Mn(II) bioadsorption, with the pseudo second order model having a better correlation with values of 0.99.

The pseudo-second order adsorption kinetics for Co(II) and Mn(II) ions at temperatures of 298, 308 and 318 K are shown in Figure 2-d and Figure 2-e, respectively. The pseudo-second order adsorption kinetics for Co(II) and Mn(II) ions at the temperatures of 298, 308 and 318 K are shown in

Figure 2-d and Figure 2-e, respectively. In Table 2, the kinetic parameters of the bioadsorption of Co(II) and Mn(II) ions are shown. It shows that the values of k and q_e were higher for the pseudo second order model, confirming its best fit. On the other hand, it was observed that the bioadsorption rate of Mn(II) ($k = 0.15 \text{ g.mg}^{-1}.\text{min}^{-1}$) is greater than Co(II) ($k = 0.026, \text{ g.mg}^{-1}.\text{min}^{-1}$), indicating that the metal ions of Mn(II) have greater mobility in solution with respect to the metal ions of Co (II). In this regard, several investigations reported that the pseudo-second order model best fits both Mn(II) (Zhang *et al.*, 2014) and Co(II) (Din *et al.*, 2013; Vilvanathan and Shanthakumar, 2015) bioadsorption data. Meanwhile, Esmaeili and Beni (2015) reported a better fit of the pseudo-first order model in the Co(II) bioadsorption.

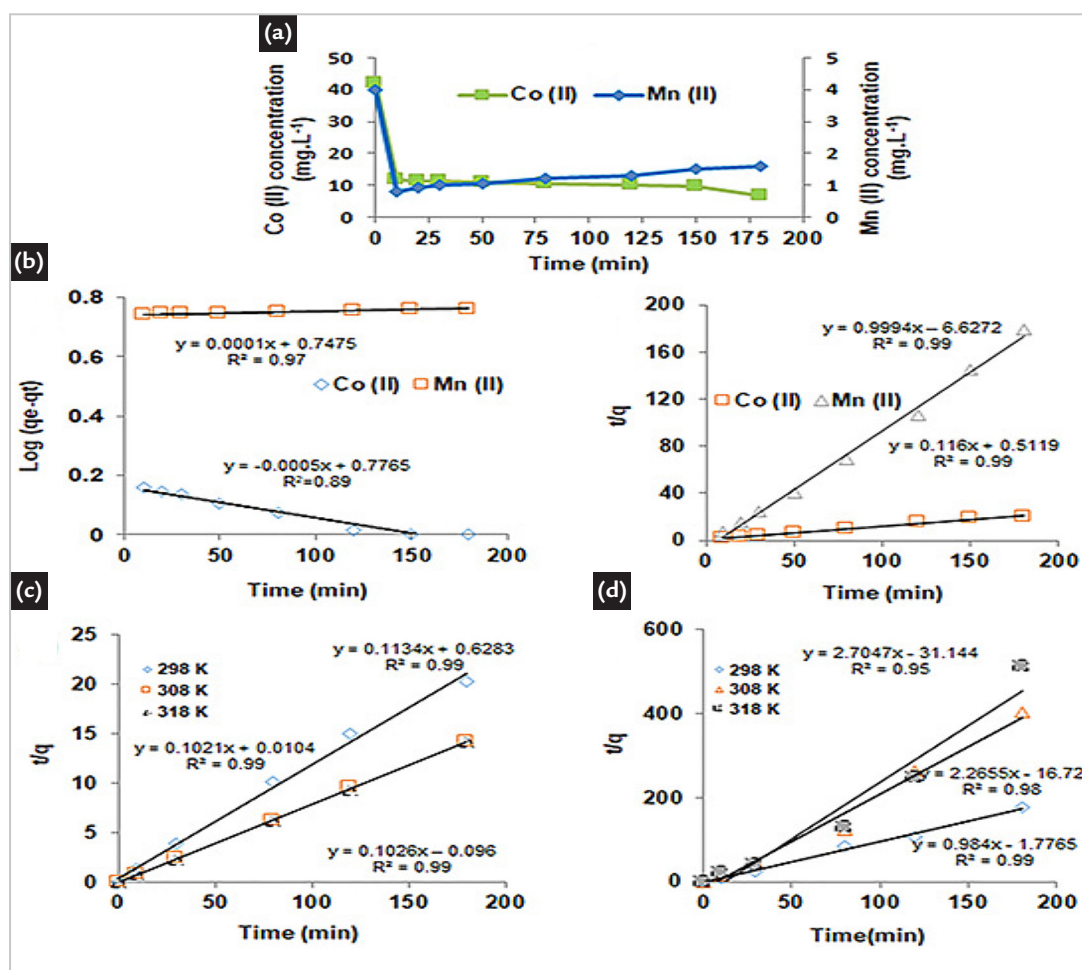


Figure 2 - a) Co(II) and Mn(II) concentration as a function of time using *R. opacus*, b) Pseudo-first order adsorption kinetic for Co(II) and Mn(II), c) Pseudo-second order adsorption kinetic for Co(II) and Mn(II), d) Pseudo-second order adsorption kinetic for Co(II) at temperatures of 298, 308 and 318 K and e) Pseudo-second order adsorption kinetic for Mn(II) at temperatures of 298, 308 and 318 K.

Table 2 - a) Kinetics parameters for Co(II) and Mn(II) bioadsorption and b) Kinetics parameters for Co(II) and Mn(II) bioadsorption using the pseudo-second order model at temperatures of 298, 308 and 318 K.

a)	Metal	q_{max} (mg.g ⁻¹)	Pseudo-first order kinetic			Pseudo-second order kinetic		
			k_1 (min ⁻¹)	q_{e1} (mg.g ⁻¹)	R^2_1	k^2 (g.mg ⁻¹ .min ⁻¹)	q_{e2} (mg.g ⁻¹)	R^2_2
	Co(II)	13.42	1.0×10^{-4}	0.11	0.89	0.026	8.62	0.994
	Mn(II)	6.9	5.0×10^{-4}	0.126	0.97	0.15	1	0.995

b)	Temperature (K)	Co(II)			Mn(II)		
		q_{e2} (mg.g ⁻¹)	k_2 (g.mg ⁻¹ .min ⁻¹)	R^2	q_{e2} (mg.g ⁻¹)	k_2 (g.mg ⁻¹ .min ⁻¹)	R^2
	298	8.82	0.02	0.99	0.21	0.15	0.99
	308	9.75	0.11	0.99	0.35	0.16	0.99
	318	9.79	1	0.99	0.43	0.21	0.98

The effect of temperature on the Co(II) and Mn(II) bioadsorption was shown in Figure 2-d and Figure 2-e, respectively. It was observed that the values of k and q are higher as the temperature increases, i.e., the bioadsorption process

is favored by the increase in the kinetic energy of the aqueous medium. Moreover, the bioadsorption rate values were higher for Mn(II) than for Co(II) because the mobility of Mn(II) is more favored with increasing temperature. Din *et al.* (2013) and

Vilvanathan and Shanthakumar (2015) also observed that Co(II) bioadsorption is favored by increasing temperature. However, Meitei and Prasad (2014) reported that there is an inverse relationship between temperature and Mn(II) ion uptake.

3.4 Thermodynamic equilibrium modeling

From the values of the bioadsorption rate constants of the pseudo-second order model presented in Table 2-b, the activation energy (E_a) of the

bioadsorption process for both metal ions was obtained using the linearized Arrhenius equation (Figure 3-a). The E_a value provides information regard-

ing the type of adsorption (physical or chemical) that occurs in the process. The Arrhenius equation is presented in Equation 6 (Tassist *et al.*, 2010).

$$K_2 = K_0 \exp\left(\frac{-E_a}{RT}\right) \quad (6)$$

Where: K_0 is the independent factor of temperature (g.mg⁻¹.min⁻¹) and R is the constant of the ideal gas law (8.314 J.mol⁻¹K⁻¹).

The E_a values of Co(II) and Mn(II) bioadsorption were 58.16 and 3.2 kJ mol⁻¹ respectively. The relatively high E_a value for the Co(II) ion indicates chemical adsorption and this was different from that reported by Din *et al.*

(2013), who obtained a lower activation energy value ($E_a = 0.007$ kJ mol⁻¹) related to physical adsorption. For the Mn(II) ion, E_a had relatively small values, suggesting the existence of physical adsorption by Van de Waals forces.

Thermodynamic parameters such as enthalpy (ΔH), Gibbs free energy (ΔG) and entropy (ΔS) variations were

estimated using variations of the equilibrium constant with temperature. These relationships were established by the Van't Hoff equation, presented in Equation 7 (Lin *et al.*, 2020; Vilvanathan and Shanthakumar, 2015). The values of ΔH and ΔS were obtained from the slope and intercept of the plot of $\ln K$ vs $1/T$.

$$\ln K = \frac{\Delta S}{R} - \frac{\Delta H}{RT} \quad (7)$$

The equilibrium constants were expressed in terms of the variation of the adsorption enthalpy as a function

of temperature using Equation 8, whereas, the Gibbs free energy and the equilibrium constant using Equation

9. The values of K_{ads} , ΔG , ΔH and ΔS are presented in Table 3.

$$\frac{d \ln K}{dT} = \frac{\Delta H}{RT^2} \quad (8)$$

$$\Delta G = -RT \ln K \quad (9)$$

Figure 3-a shows the plot of the linearized Arrhenius equation for Co(II) and Mn(II) bioadsorption. The Langmuir isotherms of the Co(II) and

Mn(II) bioadsorption process as a function of the studied temperatures (298, 308 and 318 K) are presented in Figure 3-b and Figure 3-c, respectively.

On the other hand, Figure 3-d and Figure 3-e show the plot of the Van't Hoff equation for Co(II) and Mn (II) ion adsorption, respectively.

The thermodynamic results for the bioadsorption of Co(II) ions were positive values of both ΔH and ΔS and negative value of ΔG , indicating an endothermic (chemical nature), irreversible and spontaneous process favored by increasing temperature. Positive ΔS values also indicate a decrease in randomness at the solid/solution interface

(Saleh *et al.*, 2017a; Saleh *et al.*, 2017b) or a structural change between the adsorbent and the metal (Altıntug *et al.*, 2017). Similar values of ΔG and ΔH for Co(II) bioadsorption were reported by Vilvanathan and Shanthakumar (2015) and Elanza *et al.* (2017). For the bioadsorption of Mn(II) ions, the ΔH , ΔS and ΔG values were negative, indicating an

exothermic (physical nature), reversible and spontaneous process not favored by increasing temperature. Singh *et al.* (2018) obtained positive values for both ΔH and ΔS and negative values for ΔG in Mn(II) bioadsorption, while Meitei and Prasad (2014) reported negative values for all three thermodynamic parameters evaluated.

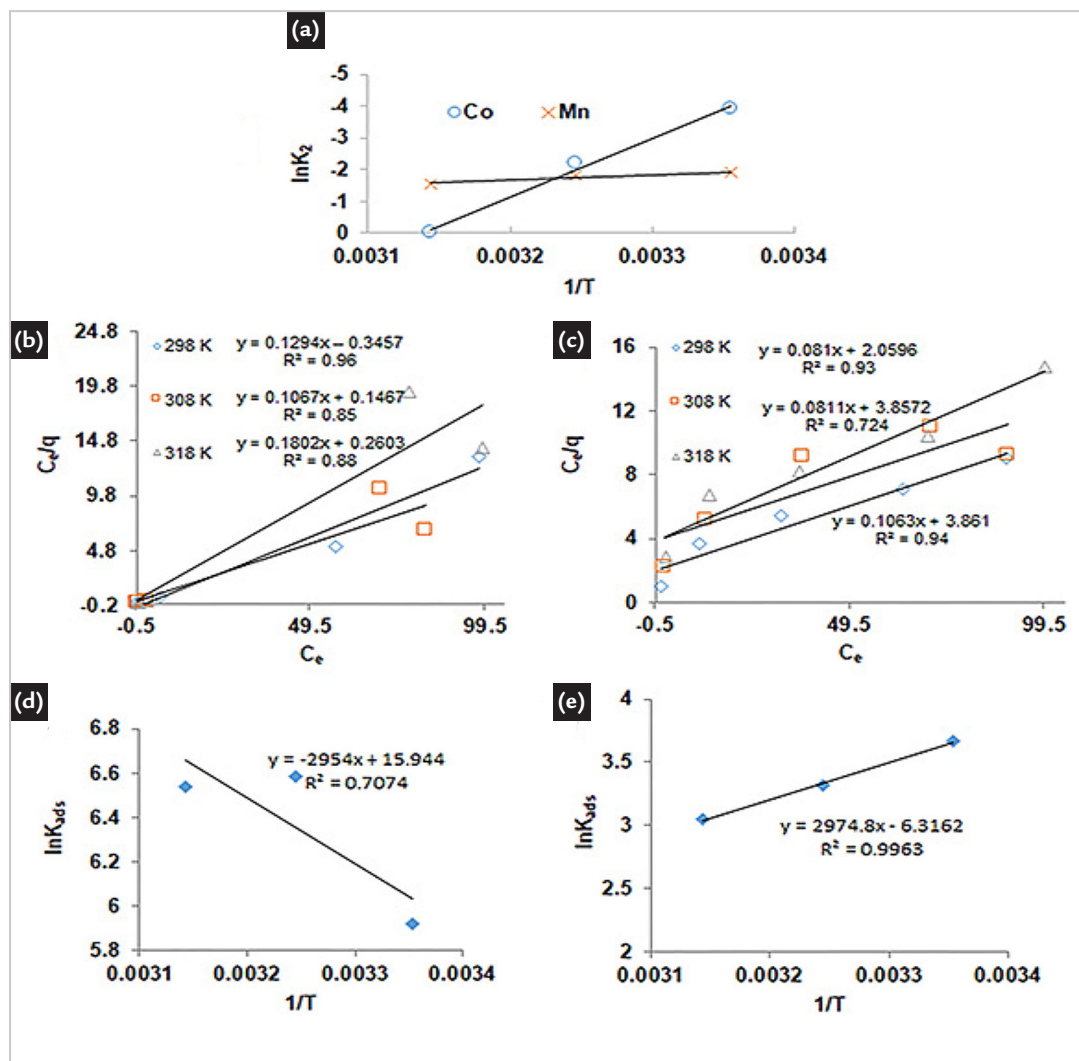


Figure 3 - a) Plot of the linearized Arrhenius equation for Co(II) and Mn(II) bioadsorption, b) Langmuir isotherm for Co(II) bioadsorption, c) Langmuir isotherm for Mn(II) bioadsorption, d) Plot of the linearized Van't Hoff equation for Co(II) bioadsorption and e) Plot of the linearized Van't Hoff equation for Mn(II) bioadsorption.

Table 3 - Thermodynamic parameters for Co (II) and Mn (II) bioadsorption as a function of temperature.

Metal	Temperature (K)	K_{ads} ($dm^3 \cdot g^{-1}$)	ΔG ($J \cdot mol^{-1}$)	ΔH ($J \cdot mol^{-1}$)	ΔS ($J \cdot mol^{-1} \cdot K^{-1}$)
Co(II)	298	374	-14685.16	2951.91	15.38
	308	727	-16880.56		
	318	692	-17297.85		
Mn(II)	298	39.33	-9102.2	-2974.8	-6.3162
	308	27.54	-8494.5		
	318	21.02	-8055.6		

4. Conclusions

The bioadsorption process of the metal ions is fast, reaching removal values of 72.3% for Co(II) and 80% for Mn(II) during the first 10 minutes. Experimental bioadsorption data for Co(II) and Mn(II) ions best fit the Langmuir model ($R^2_{\text{Co(II)}} = 0.987$ and $R^2_{\text{Mn(II)}} = 0.995$), with maximum adsorption values of 13.42 and 6.91 mg.g⁻¹,

respectively. Moreover, in the bioadsorption of Co(II) and Mn(II), there is a direct relationship between the adsorption rate and temperature, following the pseudo-second order kinetic model ($R^2_{\text{Co(II)}} = 0.994$ and $R^2_{\text{Mn(II)}} = 0.995$) with adsorption rates of 0.026 and 0.15 g.mg⁻¹.min⁻¹, respectively. On the other hand, the activa-

tion energy values showed that there is chemical adsorption for Co(II) ion and physical adsorption for Mn(II) ion. Finally, the variations of ΔG , ΔH and ΔS indicated a spontaneous, endothermic and irreversible process for the Co(II) ion and a spontaneous, exothermic and reversible process for the Mn(II) ion.

Acknowledgements

The authors would like to thank the Brazilian institutions (PUC-Rio, CNPq and

FAPERJ) and the professors of Universidad César Vallejo in Lima, Peru for their support.

References

- AL-SHAHRANI, S. S. Treatment of wastewater contaminated with cobalt using Saudi activated bentonite. *Alexandria Engineering Journal*, v. 53, n. 1, p. 205–211, 2014.
- ALTINTIG, E.; ALTUNDAG, H.; TUZEN, M.; SARI, A. Effective removal of methylene blue from aqueous solutions using magnetic loaded activated carbon as novel adsorbent. *Chemical Engineering Research and Design*, v. 122, p. 151–163, Jun. 2017.
- ARYAL, M. A comprehensive study on the bacterial biosorption of heavy metals: materials, performances, mechanisms, and mathematical modellings. *Reviews in Chemical Engineering*, v. 37, n. 6, p. 715–754, Aug. 2021.
- BENI, A. A.; ESMAEILI, A. Biosorption, an efficient method for removing heavy metals from industrial effluents: A Review. *Environmental Technology & Innovation*, v. 17, p. 100503, Feb. 2020.
- BHATTACHARYA, L.; ELZINGA, E. A Comparison of the solubility products of layered Me(II)–Al(III) hydroxides based on sorption studies with Ni(II), Zn(II), Co(II), Fe(II), and Mn(II). *Soil Systems*, v. 2, n. 2, p. 20, 2018.
- CALERO, M.; HERNÁNDEZ, F.; BLÁZQUEZ, G.; MARTIN-LARA, M. A.; TENORIO, G. Biosorption kinetics of Cd (II), Cr (III) and Pb (II) in aqueous solutions by olive stone. *Brazilian Journal of Chemical Engineering*, v. 26, n. 2, p. 265–273, 2009.
- CHENG, Q.; NENGZI, L.; BAO, L.; HUANG, Y.; LIU, S.; CHENG, X.; LI, B.; ZHANG, J. Distribution and genetic diversity of microbial populations in the pilot-scale biofilter for simultaneous removal of ammonia, iron and manganese from real groundwater. *Chemosphere*, v. 182, p. 450–457, Sep. 2017.
- CHOJNACKA, K. Biosorption and bioaccumulation - the prospects for practical applications. *Environment International*, v. 36, n. 3, p. 299–307, 2010.
- COSTA, F.; TAVARES, T. Biosorption of nickel and cadmium in the presence of diethylketone by a *Streptococcus equisimilis* biofilm supported on vermiculite. *International Biodeterioration and Biodegradation*, v. 115, p. 119–132, 2016.
- CRITTENDEN, J. C.; TRUSSELL, R. R.; HAND, D. W.; HOWE, K. J.; TCHOBANOGLIOUS, G. *MWH's water treatment: principles and design*. 3rd. ed. Hoboken, NJ, USA: John Wiley & Sons, 2012.
- DIN, M. I.; MIRZA, M. L.; ATA, S.; ATHAR, M.; MOHSIN, I. U. Thermodynamics of biosorption for removal of Co(II) ions by an efficient and ecofriendly biosorbent (*saccharum bengalense*): kinetics and isotherm modeling. *Journal of Chemistry*, v. 2, p. 11, 2013.
- DOBROWOLSKI, R.; KRZYSZCZAK, A.; DOBRZYŃSKA, J.; PODKOŚCIELNA, B.; ZIĘBA, E.; CZEMIERSKA, M.; JAROSZ-WILKOŁAZKA, A.; STEFANIAK, E. A. Extracellular polymeric substances immobilized on microspheres for removal of heavy metals from aqueous environment. *Biochemical Engineering Journal*, v. 143, p. 202–211, 15 Mar. 2019.
- EDZWALD, J. K. (ed.) *Water quality & treatment: a handbook on drinking water*. 6th. ed. [S. l.]: McGraw-Hill Education, 2011. (Water Resources and Environmental Engineering Series).
- ELANZA, S.; TAOUIL, H.; AMINE, A.; DOUBI, M.; LEBKIRI, A.; RIFI, E. L. Thermodynamic study and mathematical modeling of adsorption of Cobalt(II) ions on Biopolymers based of Sugarcane Bagasse. *Oriental Journal of Chemistry*, v. 33, n. 6, p. 3204–3210, 2017.
- ESMAEILI, A.; BENI, A. A. Biosorption of nickel and cobalt from plant effluent by *Sargassum glaucescens* nanoparticles at new membrane reactor. *International Journal of Environmental Science and Technology*, v. 12, n. 6, p. 2055–2064, 2015.
- FATHOLLAHI, A.; KHASTEGANAN, N.; COUPE, S. J.; NEWMAN, A. P. A meta-analysis of metal biosorption by suspended bacteria from three phyla. *Chemosphere*, v. 268, p. 129290, Apr. 2021.
- FOMINA, M.; GADD, G. M. Biosorption: current perspectives on concept, definition and application. *Bioresource*

- Technology*, v. 160, p. 3–14, May 2014.
- HAMIDPOUR, M.; HOSSEINI, N.; MOZAFARI, V.; HESHMATI RAFSANJANI, M. Removal of Cd(II) and Pb(II) from aqueous solutions by Pistachio Hull Waste. *Revista Internacional de Contaminación Ambiental*, v. 34, n. 2, p. 307–316, May 2018.
- HASAN, H. B.; ABDULLAH, S. R. S.; KOFLI, N. T.; YEOH, S. J. Interaction of environmental factors on simultaneous biosorption of lead and manganese ions by locally isolated *Bacillus cereus*. *Journal of Industrial and Engineering Chemistry*, v. 37, p. 295–305, 25 May 2016.
- HEJNA, M.; GOTTARDO, D.; BALDI, A.; DELL'ORTO, V.; CHELI, F.; ZANINELLI, M.; ROSSI, L. Review: Nutritional ecology of heavy metals. *Animal*, v. 12, n. 10, p. 2156–2170, 2018.
- HO, Y. S.; MCKAY, G. Pseudo-second order model for sorption processes. *Process Biochemistry*, v. 34, n. 5, p. 451–465, Jul. 1999.
- HUANG, H.; ZHAO, Y.; XU, Z.; DING, Y.; ZHANG, W.; WU, L. Biosorption characteristics of a highly Mn(II) resistant *Ralstonia pickettii* strain isolated from Mn ore. *PLoS ONE*, v. 13, n. 8, p. 1–17, 2018.
- KANAMARLAPUDI, S. L. R. K.; CHINTALPUDI, V. K.; MUDDADA, S. Application of biosorption for removal of heavy metals from wastewater. In: DERCO, J. (ed.). *Biosorption*. [S. l.]: InTech, 2018.
- KHRAISHEH, M.; AL-GHOUTI, M. A.; ALMOMANI, F. *P. putida* as biosorbent for the remediation of cobalt and phenol from industrial waste wastewaters. *Environmental Technology & Innovation*, v. 20, p. 101148, Nov. 2020.
- KOWANGA, K. D.; GATEBE, E.; MAUTI, G. O.; MAUTI, E. M. Kinetic, sorption isotherms, pseudo-first-order model and pseudo-second-order model studies of Cu (II) and Pb (II) using defatted *Moringa oleifera* seed powder. *The journal of phytopharmacology*, v. 5, n. 2, p. 71–78, 2016.
- LI, Y.; XU, Z.; MA, H.; HURSTHOUSE, A. S. Removal of manganese(II) from acid mine wastewater: a review of the challenges and opportunities with special emphasis on Mn-oxidizing bacteria and microalgae. *Water*, v. 11, n. 12, p. 2493, 26 Nov. 2019.
- LIN, Z.; YUAN, P.; YUE, Y.; BAI, Z.; ZHU, H.; WANG, T.; BAO, X. Selective adsorption of Co(II)/Mn(II) by zeolites from purified terephthalic acid wastewater containing dissolved aromatic organic compounds and metal ions. *Science of the Total Environment*, v. 698, p. 134287, 2020.
- MATSUSHITA, S.; KOMIZO, D.; CAO, L. T. T.; AOI, Y.; KINDAICHI, T.; OZAKI, N.; IMACHI, H.; OHASHI, A. Production of biogenic manganese oxides coupled with methane oxidation in a bioreactor for removing metals from wastewater. *Water Research*, v. 130, p. 224–233, Mar. 2018.
- MEITEI, M. D.; PRASAD, M. N. V. Adsorption of Cu (II), Mn (II) and Zn (II) by *Spirodela polyrhiza* (L.) Schleiden: equilibrium, kinetic and thermodynamic studies. *Ecological Engineering*, v. 71, p. 308–317, 2014.
- OZDEMIR, S.; KILINÇ, E.; FATİH, S. A novel biosorbent for preconcentrations of Co(II) and Hg(II) in real samples. *Scientific Reports*, v. 10, n. 1, p. 1–9, 2020.
- PARK, D.; YUN, Y. S.; PARK, J. M. The past, present, and future trends of biosorption. *Biotechnology and Bioprocess Engineering*, v. 15, n. 1, p. 86–102, 2010.
- PATIL, D. S.; CHAVAN, S. M.; OUBAGARANADIN, J. U. K. A review of technologies for manganese removal from wastewaters. *Journal of Environmental Chemical Engineering*, v. 4, n. 1, p. 468–487, 2016.
- PIMENTEL, A. M. R. *Remoção de Co(II) e Mn(II) de soluções aquosas utilizando a biomassa R. opacus*. 2011. Dissertação (Mestrado) – Departamento de Engenharia de Materiais, Pontifícia Universidade Católica do Rio de Janeiro, Rio de Janeiro, 2011.
- QIAO, W.; ZHANG, P.; SUN, L.; MA, S.; XU, W.; XU, S.; NIU, Y. Adsorption performance and mechanism of Schiff base functionalized polyamidoamine dendrimer/silica for aqueous Mn(II) and Co(II). *Chinese Chemical Letters*, n. 2019, 2020.
- ROSSI, L.; FUSI, E.; BOGLIONI, M.; GIROMINI, C.; REBUCCI, R.; BALDI, A. Effect of zinc oxide and zinc chloride on human and swine intestinal epithelial cell lines. *International Journal of Health, Animal Science and Food Safety*, v. 1, n. 2, p. 1–7, 2014.
- SALEH, T. A.; SARI, A.; TUZEN, M. Effective adsorption of antimony(III) from aqueous solutions by polyamide-graphene composite as a novel adsorbent. *Chemical Engineering Journal*, v. 307, p. 230–238, Jan. 2017a.
- SALEH, T. A.; TUZEN, M.; SARI, A. Magnetic activated carbon loaded with tungsten oxide nanoparticles for aluminum removal from waters. *Journal of Environmental Chemical Engineering*, v. 5, n. 3, p. 2853–2860, Jun. 2017b.
- SINGH, J.; DHIMAN, N.; SHARMA, N. K. Effect of Fe(II) on the adsorption of Mn(II) from aqueous solution using esterified saw dust: equilibrium and thermodynamic studies. *Indian Chemical Engineer*, v. 60, n. 3, p. 255–268, 2018.
- TASSIST, A.; LOUNICI, H.; ABDI, N.; MAMERI, N. Equilibrium, kinetic and thermodynamic studies on aluminum biosorption by a mycelial biomass (*Streptomyces rimosus*). *Journal of Hazardous Materials*, v. 183, n. 1–3, p. 35–43, 2010.
- THIRULOGACHANDAR, A.; RAJESWARI, M.; RAMYA, S. Assessment of heavy metals in gallus and their impacts on human. *International Journal of Scientific and Research Publications*, v. 4, n. 6, p. 1–8, 2014.
- VILVANATHAN, S.; SHANTHAKUMAR, S. Biosorption of Co(II) ions from aqueous solution using *Chrysanthemum indicum*: kinetics, equilibrium and thermodynamics. *Process Safety and Environmental Protection*, v. 96, n. 1i, p. 98–110, 2015.

WEBER, T. W.; CHAKRAVORTI, R. K. Pore and solid diffusion models for fixed-bed adsorbers. *AIChE Journal*, v. 20, n. 2, p. 228–238, Mar. 1974.

ZHANG, Y.; ZHAO, J.; JIANG, Z.; SHAN, D.; LU, Y. Biosorption of Fe(II) and Mn(II) ions from aqueous solution by rice husk ash. *BioMed Research International*, v. 2014, n. 2, p. 10, 2014.

Received: 10 October 2020 - Accepted: 3 December 2021.



All content of the journal, except where identified, is licensed under a Creative Commons attribution-type BY.